

Measurement report: Hydrolyzed Amino acids in fine and coarse atmospheric aerosol in Nanchang, China: concentrations, compositions, sources and possible bacterial degradation state

5 Ren-guo Zhu¹, Hua-Yun Xiao^{2*}, Li Luo¹, Hongwei Xiao¹, Zequn Wen³, Yuwen Zhu^{1,4}, Xiaozheng Fang¹, Yuanyuan Pan¹, Zhenping Chen¹

¹Jiangxi Province Key Laboratory of the Causes and Control of Atmospheric Pollution, East China University of Technology, Nanchang 330013, China.

10 ²School of Environmental Science and Engineering, Shanghai Jiao Tong University, Shanghai 200240, China

³Department of Earth Sciences, Faculty of Land Resource Engineering, Kunming University of Science and Technology, Kunming 650021, China

⁴School of Earth Sciences, East China University of Technology, Nanchang 330013, China;

Corresponding author: Hua-Yun Xiao (xiaohuayun@ecut.edu.cn)

15 **Abstracts.** Amino acids (AAs) are relevant for nitrogen cycles, climate change and public health. Their size distribution may help to uncover the source, transformation and fate of protein in the atmosphere. This paper explores the use of compound-specific $\delta^{15}\text{N}$ patterns of hydrolyzed amino acid (HAA), $\delta^{15}\text{N}$ values of total hydrolyzed amino acid ($\delta^{15}\text{N}_{\text{THAA}}$), degradation index (DI), and the variance within trophic AAs ($\sum V$) as markers to examine the sources and processing history of different sizes particle in the atmosphere. 2-weeks of daily aerosol samples from five sampling sites in the Nanchang area (Jiangxi Province, China) and samples of main emission sources of AAs in aerosols (biomass burning, soil and plants) were collected (Zhu et al., 2020). Here, we measured the concentrations and $\delta^{15}\text{N}$ values of each HAA in two size segregated aerosol particles ($>2.5\mu\text{m}$ and $\text{PM}_{2.5}$). Our results showed that the average concentrations of THAA in fine particles was nearly 6 times higher than that in coarse particles ($p<0.01$) and composition profiles of fine and coarse particles were quite different from each other. The $\delta^{15}\text{N}$ values of hydrolyzed glycine and THAA in both fine and coarse particles were typically in the range of those from biomass burning, soil and plant sources. Moreover, the average difference in the $\delta^{15}\text{N}_{\text{THAA}}$ value between fine and coarse particles was smaller than 1.5%. These results suggested that the sources of atmospheric HAAs for fine and coarse particles might be similar. Meanwhile, compared to fine particles, significantly lower DI values ($p<0.05$), “scattered” $\delta^{15}\text{N}$ distribution in Trophic-AA and higher $\sum V$ values ($p<0.05$) were observed in coarse particles. But the difference in $\delta^{15}\text{N}$ values of Source-AA (glycine, serine, phenylalanine and lysine) and THAA between coarse particles and fine particles was relatively small. It is likely that AAs in coarse particles have advanced bacterial degradation state compared to fine particles. Besides that, the significant increase in DI values and a decrease in $\sum V$ values for coarse particles were observed during the rainfall events ($p<0.05$). This implies that “fresh” AAs in coarse particles were mainly released following the precipitation.

20
25
30
35

1 Introduction

Recently, an increasing number of researchers highlight the importance of amino acids (AAs) in the atmosphere because AA is considered to be one of the most important organic nitrogen compounds in atmosphere (Zhang et al., 2002; Matos et al., 2016). Moreover, AAs are bioavailable and can be directly utilized by plant and soil communities (Wedyan and Preston, 2008; Song et al., 2017). Its key role in atmosphere-biosphere nutrient cycling and global nitrogen cycle has aroused greatly concern (Samy et al., 2013; Zhang and Anastasio, 2003). Besides that, AAs and proteins are important constituents of allergenic bioaerosol (Miguel et al., 2009; Huffman et al., 2013). The distribution of AAs and proteins in different particle sizes will determine whether these compounds can reach the pulmonary alveoli and the allergenicity of aerosols (Di Filippo et al., 2014). And the distribution of AAs associated with different particle sizes can help to trace the sources and transformation of atmospheric aerosols (Barbaro et al., 2019; Feltracco et al., 2019; Di Filippo et al., 2014).

The sources of atmospheric proteinaceous matter are very complex. Primary biological aerosol particles (e.g, plants, soil, pollen, bacteria, fungi, spores and deris of living things), biomass burning, and agricultural activities are generally suggested to be the main contributing sources of atmospheric AAs (Matos et al., 2016; Mace et al., 2003). It is still unclear whether AAs fine and coarse particles influenced by different sources.

Compound-specific nitrogen isotope analysis of individual amino acids provide an opportunity to offer the key information on widely varied photochemical processes and origins of proteinaceous matter in the atmosphere. Nitrogen sources information and any possible nitrogen isotopic fractionation caused by transformation processes could be hold by the $\delta^{15}\text{N}$ -AA pattern (Mccarthy et al., 2007; Bol et al., 2002). At the same time, the $\delta^{15}\text{N}$ value of total hydrolysable AA ($\delta^{15}\text{N}_{\text{Avg-THAA}}$), calculated as the average molar-weighted $\delta^{15}\text{N}$ value of individual AA, has been used as a proxy for total protein $\delta^{15}\text{N}$ value (Mccarthy et al., 2013). However, to our knowledge, no study has used the $\delta^{15}\text{N}$ -AA pattern and $\delta^{15}\text{N}_{\text{Avg-THAA}}$ values to identify the sources of AAs distributed in different particle sizes.

It is generally accepted that AAs in aerosols are mainly controlled by abiotic photochemical aging processes. On the contrary, the biological degradation of AAs in aerosols are neglected. This can be attributed to two factors. First, the sources and transformation pathways of protein matter and AAs in aerosols are highly complex (Wang et al., 2019; Zhu et al., 2020). Second, and the residence time of protein matter in aerosols is relatively short (Papastefanou, 2006). Admittedly, bacteria and fungi are ubiquitous and can be observed in all PM samples where people look for them, and this has been done routinely for many decades (Bauer et al., 2002; Bowers et al., 2013; Huffman et al., 2013; Wei et al., 2016; Wei et al., 2019). *In-situ* bacterial degradation processes occurred in the aerosols and the cloud water was also observed (Amato et al., 2007; Husárová et al., 2011). Unfortunately, bacterial degradation of atmospheric AAs is limited. For example, two studies on marine aerosols by Wedyan and Preston (2008) and Kuznetsova et al. (2005), and one study on precipitation by Yan et al. (2015). The degradation index (DI) proposed by Dauwe et al. (1998, 1999) has been wildly used to assess the degradation state of organic materials (OM) in terrestrial, aquatic, and marine environment (Dauwe and Middelburg, 1998; Wang et al., 2018; Dauwe et al., 1999). This value is based on the molar percentage (Mol%) of the amino acid pool and higher DI values denote a more “fresh” state of protein matter. However, DI values of AAs

in aerosol particles and whether bacterial degradation plays a role in the levels and compositions of AAs in different particle sizes are still unknown.

80 A consensus has recently been reached on selective use of the ^{15}N depleted or enriched trophic AAs during bacterial heterotrophy processes can lead to large nitrogen isotopic fractionation in trophic AAs (McCarthy et al., 2004). Thus, substantial $\delta^{15}\text{N}$ pattern shifts of trophic AAs can index bacterial heterotrophy processes. $\sum V$, defined as the average deviation in the $\delta^{15}\text{N}$ values of the Tr-AA, has therefore been established to track the degree of bacterial degradation of AAs in marine and terrestrial environment (Mccarthy et al., 2007;Philben et al., 2018;Yamaguchi et al., 2017).

85 In the present work, we sought to improve our understanding of AAs distributed in different particle sizes. We measured the concentrations and $\delta^{15}\text{N}$ values of each hydrolyzed amino acid in two size segregated aerosol particles ($>2.5\ \mu\text{m}$ and $\text{PM}_{2.5}$) in aerosols collected in the Nanchang area (southeastern China). Furthermore, $\delta^{15}\text{N}$ values of Gly and THAA in fine and coarse particle were compared with those in main emission sources (biomass burning, soil and plant sources) to identify the potential sources of fine and coarse particles. In addition, the DI, $\sum V$ values and $\delta^{15}\text{N}$ values pattern of hydrolyzed AA in fine and coarse particles were analyzed to explore the possible bacterial degradation of HAAs in fine and coarse particles.

2 Experimental section

2.1 Sample collection

95 Aerosol samples were collected at 5 locations included urban, town, suburban, agricultural area and forest in Nanchang area (South China) from April 30, 2019 to May 13, 2019, using a high-volume air sampler (KC-1000, Qingdao Laoshan Electronic Instrument company, China) at a flow rate of $1.05 \pm 0.03\ \text{m}^3\ \text{min}^{-1}$. The Characteristics of 5 sampling area were defined in Table S1. The sampler allows to separate particles of different aerodynamic diameters in two stages with diameter (D) above $2.5\ \mu\text{m}$ (coarse particles) and $D \leq 2.5\ \mu\text{m}$ (fine particles). Quartz fiber filters were used and filters were heated at 450°C for 10 h to remove any organics before sampling. Aerosol sampling was conducted at the rooftop of the building in each site, about 10 meters above the ground except for the agricultural area where the sampler was placed in a clear spot about 1000 meters away from the runway. The sampling time for each sample was from 5 p.m. to 4:30 p.m. of next day. More details on the sample collection are provided in Zhu et al. (2020).

105 Forest soil samples were collected at the top 10-cm of the evergreen broad-leaved forest soil in Nanchang area (115.8°E , 28.8°N). Paddy soil samples were collected from the topmost 10-cm layer of rice cultivation soil (115.1°E , 28.2°N). Road soil was collected from highway topsoil (115.8°E , 28.7°N). For each type of soil samples, triplicate representative soil samples (approximately 100 g) were collected.

110 Masson pine (*Pinus massoniana* (Lamb.)) and camphor (*Cinnamomum Camphora*) tree as a common vegetation in the study area (115.8°E , 28.8°N) were collected during May 2019. Approximately 4-6 g of pine needles or camphor leaves were collected from the outer branches in the east, south, north, and west directions (about 10 m above the ground). We collected 5-6 representative samples for each kind of leaves. All fresh samples were placed in plastic bags, labeled and stored in a chilled box immediately. In the

115 laboratory, all plant and soil samples were freeze-dried. Then, freeze-dried samples were stored at -80°C until further use.

Aerosols from straw burning were sampled by pumping into a high-volume air sampler (KC-1000, Qingdao Laoshan Electronic Instrument Company, China) from the funnel on the combustion furnace during July 2017. The combustion furnace is a domestic furnace widely used by local residents.

120 **2.2 Analyses of the concentration and $\delta^{15}\text{N}$ value of individual hydrolyzed amino acid (HAA)**

For hydrolyzed AA analysis, samples were prepared using a modified version of Wang et al. (2019) and Ren et al. (2018). One-sixteenth of each fine aerosol filter ($\sim 80\text{ m}^3$ of air) or Two-seventh of each coarse aerosol filter ($\sim 366\text{ m}^3$ of air) was broken into small pieces and placed in a glass hydrolysis tube. Prior to the hydrolysis, $25\ \mu\text{L}$ of ascorbic acid at a concentration of $20\ \mu\text{g}\ \mu\text{L}^{-1}$ ($500\ \mu\text{g}$ absolute) was added to
125 each filter sample. Then, 10 mL and 6 M Hydrochloric acid (HCl) was used to convert all of the combined AAs to free AAs. To avoid oxidation of AAs, the hydrolysis tube was flushed with nitrogen and tightly sealed before hydrolysis. The mixture was later placed in an oven at $110\ ^{\circ}\text{C}$ for 24 h.

For plant and soil samples, approximately $30\text{--}40\text{ mg}$ of plant or $500\text{--}600\text{ mg}$ of soil were ground separately in liquid nitrogen into fine powders using a mortar and pestle. Then, well ground and homogenized soil
130 and plant power were hydrolyzed in the same way as the aerosol samples.

After cooling to room temperature, the hydrolyzed solution was dried with a stream of nitrogen and HCl was removed. The dried solution was then redissolved in $0.1\ \text{M}$ HCl and purified by a cation exchange column (Dowex 50W X 8H^+ , 200-400 mesh; Sigma-Aldrich, St Louis, MO, USA). Later, tert-Butyldimethylsilyl (tBDMS) derivatives of HAAs were prepared following the method described by our
135 previous study Zhu et al. (2018).

The concentrations of HAAs were analyzed using a gas chromatograph-mass spectrometer (GC-MS). The GC-MS instrument was composed of a Thermo Trace GC (Thermo Scientific, Bremen, Germany) connected into a Thermo ISQ QD single quadrupole MS. The single quadrupole MS was operated in electron impact ionization ($70\ \text{eV}$ electron energy) and full scan mode. The temperatures of the transfer
140 line and ion source were 250°C and 200°C , respectively. More details on quality assurance and control (recoveries, linearity, detection limits, quantitation limits, and corresponding effective limits in the aerosol samples of AAs), are provided in Zhu et al. (2020)

$\delta^{15}\text{N}$ values of AA-tert-butyl dimethylsilyl (tBDMS) derivatives were analyzed using a Thermo Trace GC (Thermo Scientific, Bremen, Germany) and a conflo IV interface (Thermo Scientific, Bremen,
145 Germany) interfaced with a Thermo Delta V IRMS (Thermo Scientific, Bremen, Germany). The analytical precision (SD, $n=3$) of $\delta^{15}\text{N}$ was better than $\pm 1.4\text{‰}$. Moreover, AABA with known $\delta^{15}\text{N}$ value ($-8.17\text{‰}\pm 0.03\text{‰}$) was added in each sample to check the accuracy of the isotope measurements. The analytical run was accepted when the differences of $\delta^{15}\text{N}$ values of AABA between GC- IRMS and EA-IRMS values were at most $\pm 1.5\text{‰}$. Each reported value is a mean of at least three $\delta^{15}\text{N}$ determinations.

150 For more details of the analyses of HAA $\delta^{15}\text{N}$ values refer to our previous publication (Zhu et al., 2018). The concentrations and $\delta^{15}\text{N}$ value of Cys, Trp, Asn and Gln in HAAs could not be determined using this method because, under strong acidic condition, Cys and Trp is destroyed, and Asn and Gln are converted to Asp and Glu, respectively. The concentration and $\delta^{15}\text{N}$ value of hydrolysable Asp represents the sum

of Asp and Asn; the concentration and $\delta^{15}\text{N}$ value of hydrolysable Glu represents the sum of Glu and Gln.

155 2.3 DI index

Degradation process could significantly modify the mole composition of protein amino acids (Dauwe et al., 1999). Accordingly, a quantitative degradation index (DI) has been developed based on the mole composition of hydrolyzed amino acids pool. The degradation index (DI) was calculated using the formula Eq. (1) originally proposed by Dauwe et al. (1999):

$$160 \quad \text{DI} = \sum_i \left(\frac{\text{Var}_i - \text{Avg}_i}{\text{SD}_i} \right) \times \text{PC1}_i \quad (1)$$

where DI is the degradation index, Var is the mole% of the each individual HAA, Avg_{*i*}, and SD_{*i*} are the average mole% and standard deviation of each HAA in our data set, respectively, and PC1 is the loading of the amino acid *i* obtained from principal component analysis (Table S2).

2.4 $\delta^{15}\text{N}$ values

165 The natural abundance of ^{15}N was calculated as $\delta^{15}\text{N}$ values in per mil (‰), using atmospheric N_2 as the international standard:

$$\delta^{15}\text{N} (\text{‰ vs air}) = \left(\frac{R_{\text{sample}}}{R_{\text{standard}} - 1} \right) \times 1000 \quad (2)$$

where R is the ratio of mass 29/mass 28.

170 A derivatized mixture of 20 amino acid standards (Ala, Gaba, Arg, Asn, Asp, Gln, Glu, Gly, His, Ile, Leu, Lys, Met, Phe, Pro, Ser, Thr, Trp, Tyr, and Val) and several international amino acid standards (Ala, Gly3, Gly4, Phe, USGS40, USGS41a, and Val) with known $\delta^{15}\text{N}$ values (−26.35 to +47.55‰) was prepared to assess the isotope measurement reproducibility and normalize the $\delta^{15}\text{N}$ values of the amino acids in the samples (Zhu et al., 2018).

2.5 $\sum V$ parameter

175 The $\sum V$ parameter is defined as the average absolute deviation in the $\delta^{15}\text{N}$ values of the Trophic AA (including: Ala, Asp, Glu, Ile, Leu, and Pro) (Mccarthy et al., 2007). This parameter has been used as a proxy for the degree of heterotrophic resynthesis and calculated by Eq. (3):

$$\sum V = \frac{1}{n} \times \sum \text{Abs}(\chi_{\text{AA}}) \quad (3)$$

180 where χ_{AA} is defined as the deviation of the $\delta^{15}\text{N}$ of each trophic amino acid from the $\delta^{15}\text{N}$ of the mean of trophic amino acids ($\delta^{15}\text{N}_{\text{AA}}$ - average $\delta^{15}\text{N}$ of Ala, Asp, Glu, Ile, Leu, and Pro), and n is the total number of trophic amino acids used in the calculation.

2.6 $\delta^{15}\text{N}_{\text{THAA}}$ values

The $\delta^{15}\text{N}$ values of total hydrolysable amino acids ($\delta^{15}\text{N}_{\text{THAA}}$) is calculated as the mole percent weighted sum of the $\delta^{15}\text{N}$ values of each individual HAA, following Eq. (4):

$$185 \quad \delta^{15}\text{N}_{\text{THAA}} = \sum (\delta^{15}\text{N}_{\text{HAA}} \cdot \text{mol\%HAA}) \quad (4)$$

Where mol%HAA is the mole contribution of each HAA and $\delta^{15}\text{N}_{\text{THAA}}$ is the $\delta^{15}\text{N}$ value of individual HAA.

2.7 Statistics

All statistical analyses were performed using SPSS 16.0 (SPSS Science, USA). Graphs were generated using OriginPro 2018 (OriginLab Corporation, USA) and Sigmaplot 12.5 software (SPSS Science, USA). We performed a Two-way ANOVA for the concentration of THAA, the DI index, $\delta^{15}\text{N}_{\text{THAA}}$ values and $\sum V$ values, testing the effect of aerosol sizes, location, and their interaction. Tukey's Honestly Significant Differences (Tukey-HSD) test was used to evaluate which combinations of location and aerosol size were significantly different. Two-way ANOVA was also conducted for DI values, examining the effect of aerosol sizes, coefficients (obtained by using first principal component score or previous reported coefficients) and their interaction. The differences in $\delta^{15}\text{N}_{\text{Gly}}$ values for fine particles between 5 sampling locations were examined using the one-way analysis of variance (ANOVA) procedure, and compared using the Tukey-HSD test.

The exponential regression was analyzed to evaluate changes in DI index as a function of the concentration of THAA.

To test for changes in the concentration of THAA, DI index and $\sum V$ values following the rain events, a two-way ANOVA was performed, testing for effects of precipitation, aerosol sizes and their interactions. Tukey-HSD test was conducted to compare the significant difference. Changes in mol% of each HAAs concentrations following precipitation were tested for significance by using ANOVA procedure followed by a Tukey-HSD test to compare significant differences. For all tests, statistically significant differences were considered at $p < 0.05$.

3 Results and discussion

3.1 Concentrations and mol% composition profile of HAA in size-segregated aerosol

Fourteen hydrolyzed amino acids (Ala, Val, Leu, Ile, Pro, Gly, Ser, Thr, Phe, Asp, Glu, Lys, His and Tyr) were found in fine and coarse aerosol samples collected in Nanchang areas during spring 2019 (Fig. 1). The average concentrations of THAA in fine and coarse particles were $2542 \pm 1820 \text{ pmol m}^{-3}$ and $434 \pm 722 \text{ pmol m}^{-3}$, respectively. The mean concentration of THAA for fine particles was nearly 6 times higher than that for coarse particles ($p < 0.01$) (Fig. S1).

For fine particles, the average concentration of THAA in 5 sampling sites were significantly different ($p < 0.05$), with the highest mean concentration of THAA in agricultural area ($3455 \pm 2203 \text{ pmol m}^{-3}$), followed by those in urban ($2941 \pm 2443 \text{ pmol m}^{-3}$), forest ($2730 \pm 1435 \text{ pmol m}^{-3}$) and town ($2314 \pm 1211 \text{ pmol m}^{-3}$). The lowest THAA concentration occurred at suburban ($1633 \pm 1087 \text{ pmol m}^{-3}$) (Fig. S1).

However, for coarse particles, the difference in THAA concentrations between 5 sampling sites were not significant ($p > 0.05$) (Fig. S1). The mean concentration of THAA in agricultural area, urban, forest, town and suburban location was $540 \pm 821 \text{ pmol m}^{-3}$, $230 \pm 300 \text{ pmol m}^{-3}$, $654 \pm 1152 \text{ pmol m}^{-3}$, $437 \pm 583 \text{ pmol m}^{-3}$ and $291 \pm 426 \text{ pmol m}^{-3}$, respectively. The highest concentration of atmospheric AAs at the agricultural area would be ascribed to the enhanced agricultural activities and natural source emission (e.g., pollen grain) in spring (Xu et al., 2019).

The composition profiles of HAA in fine and coarse particles during the whole campaign are shown in

Fig. 2. The composition profiles of HAA in fine particles are quite different from those in coarse particles (Fig. 2). For fine particles, Gly, Pro, Leu and Glu were the four most abundant compounds, accounting for an average of $25 \pm 12\%$, $17 \pm 8\%$, $12 \pm 3\%$ and $11 \pm 6\%$, respectively, of the THAA pool.

For coarse particles, Pro were the most abundant THAA specie, with an average contribution of $63 \pm 31\%$ to the THAA pool. Leu, Ala and Val were the next most abundant species, each accounting for 7-9% of the THAA pool, while other individual HAA was only minor component in coarse particles (Fig. 2 and Fig. 2). The HAA distribution among the different sampling locations for both fine and coarse particles appeared similar (Fig. 2).

3.2 Similar contribution sources of fine and coarse particles

The detailed size-resolved investigation for the sources of atmospheric AAs is limited. Filippo et al. (2014) obtained very variable results for the size-segregated concentrations of atmospheric combined amino acids in the city Rome. In the warm season, highest concentration of CAAs distributed in the fine fraction, whereas, in the colder season, the increase distribution of CAAs in the coarse fractions was observed. Feltracco et al. (2019) demonstrated that free and combined amino acids in Arctic aerosol were mainly distributed in fine fraction, which could be affect by several sources, including biological primary production and biomass burning. These results could not provide conclusive evidence to define the origin of atmospheric AAs in the different particle sizes.

With the development of stable N isotope technology, $\delta^{15}\text{N}$ values and $\delta^{15}\text{N}$ pattern has become effective tools to trace the sources of nitrogen compounds. Our previous study found that the $\delta^{15}\text{N}$ value of Gly in PM_{2.5} can be used to trace the potential emission sources for aerosol AAs because the N isotope fractionation associated with Gly transformation in aerosol is relatively small (Zhu et al., 2020). To trace the sources of fine and coarse particles, we measured the nitrogen isotopic compositions of hydrolyzed Gly and THAA sampled from main emission sources in the study areas, including biomass burning, soil and local plants (Fig. 3). The average $\delta^{15}\text{N}$ value for hydrolyzed Gly from the biomass burning, soil, and plant sources was $+15.6 \pm 4.3\%$, $+3.0 \pm 4.4\%$, and $-11.9 \pm 1.4\%$, respectively, and the mean $\delta^{15}\text{N}_{\text{THAA}}$ value was $+15.8 \pm 4.5\%$, $+5.5 \pm 2.2\%$, and $-0.0 \pm 1.8\%$, respectively.

In this study, the $\delta^{15}\text{N}$ values of hydrolyzed Gly in fine and coarse particles exhibited wide ranges: -1.0% to $+20.3\%$ and -0.8% to $+15.7\%$, which fall within the ranges of biomass burning, soil, and plants sources (Fig. 3). The $\delta^{15}\text{N}$ of protein AA ($\delta^{15}\text{N}_{\text{THAA}}$) has been also served as a proxy for indicating the nutrient N in marine sediments (Batista et al., 2014). To test $\delta^{15}\text{N}_{\text{THAA}}$ values of aerosol particles could also be used to trace the sources of aerosol particles, $\delta^{15}\text{N}_{\text{THAA}}$ values were compared with the $\delta^{15}\text{N}_{\text{Gly}}$ values. Since the concentration of hydrolyzed Gly is very low in coarse particles, a few the $\delta^{15}\text{N}_{\text{Gly}}$ values could be measured in coarse aerosol samples. Thus, only the $\delta^{15}\text{N}_{\text{THAA}}$ values of fine particles were compared with the $\delta^{15}\text{N}_{\text{Gly}}$ values of fine particles in the same sampling sites.

A remarkably consistent spatial-related trend was observed in $\delta^{15}\text{N}_{\text{THAA}}$ values and the $\delta^{15}\text{N}$ values of hydrolyzed Gly (Fig. 4b and 4c). Both $\delta^{15}\text{N}_{\text{Gly}}$ values and the $\delta^{15}\text{N}_{\text{THAA}}$ values of fine particles in the urban and town locations showed more positive than those in suburban, agricultural area and forest locations ($p < 0.05$). Furthermore, the mean $\delta^{15}\text{N}_{\text{THAA}}$ value was not significantly different from the average $\delta^{15}\text{N}$ value of hydrolyzed Gly in the 5 sampling locations ($p > 0.05$), supporting $\delta^{15}\text{N}_{\text{THAA}}$ values

265 of aerosols may also imprint the sources of atmospheric AAs. Similarly, according to the $\delta^{15}\text{N}$ inventories of THAA in potential emission sources of atmospheric protein AA, both fine (+0.7‰ to +13.3‰) and coarse particles (-2.3‰ to +10.0‰) had the $\delta^{15}\text{N}_{\text{THAA}}$ value also typically in the range of these three main emission sources (Fig. 3). Therefore, it is likely that the main sources of atmospheric AAs for both fine and coarse particles were mainly biomass burning, soil, and plants.

270 However, there is no significant difference in the $\delta^{15}\text{N}_{\text{THAA}}$ value between fine and coarse particles in each sampling sites ($p>0.05$) (Fig. 4c) and the average offset of $\delta^{15}\text{N}_{\text{THAA}}$ value between fine and coarse particles was lower than $1.5 \pm 1.7\%$ at 5 sampling sites (Fig. 4a). Thus, it is suggested that the main sources of AAs in fine and coarse particles might be similar, all of which were influenced by biomass burning, soil, and plant sources.

275 In addition, as one of the main components of primary biological aerosol particles (PBAP), AAs are proved to be ejected from ocean water by bursting bubbles (Leck and Bigg, 2005a, 2005b; Bigg, 2007; Bigg and Leck, 2008). Marine source may also contribute to atmospheric AAs for both fine and coarse particles observed here. However, the sampling sites are located in an inland city. Considering the 2-day back trajectory of during sampling periods (Fig. S2), we can observe that the aerosol collected flowed
280 principally from the mainland and air mass from marine only accounted for 16%. Moreover, during the long transport, PBAP may be removed by dry and wet deposition (Després et al., 2012). Therefore, in this study, compared to land origin, the contribution of marine source to aerosol AAs observed here may be relatively small. Unfortunately, we do not have $\delta^{15}\text{N}$ -HAA data for marine aerosols. Pooled $\delta^{15}\text{N}_{\text{Gly}}$ values from literature data, we found the $\delta^{15}\text{N}_{\text{Gly}}$ values in ocean high molecular weight dissolved organic matter, cyanobacteria and plankton ranged from -16.6‰ to +7.7‰ (McCarthy et al., 2007; Mcclelland and Montoya, 2002; Chikaraishi et al., 2009; Calleja et al., 2013), which was close to the range of the natural source including plant (range: -13.2‰ to -9.7‰) and soil (range: -1.6‰ to +7.4‰) sources.
285 Conclusively, the contribution from soil and plant sources mentioned in this study may include a very small amount of marine contribution.

290 3.3 Sources of HAA in aerosol at different locations

The $\delta^{15}\text{N}_{\text{Gly}}$ values of fine particles was significantly different at 5 sampling sites ($p<0.05$). The average $\delta^{15}\text{N}_{\text{Gly}}$ value of fine particles in urban (average= $14.3 \pm 8.5\%$) and town (average= $9.4 \pm 4.2\%$) were more positive than that in suburban (average= $6.7 \pm 4.3\%$), agricultural area (average= $6.9 \pm 5.3\%$) and forest site (average= $6.5 \pm 5.0\%$) (Fig. 4b). The significantly higher $\delta^{15}\text{N}_{\text{Gly}}$ values observed in the urban
295 and town locations suggested an increased contribution from biomass burning sources to Gly in fine particles at these two locations.

Similar spatial variation trend in $\delta^{15}\text{N}_{\text{THAA}}$ values of fine and coarse particles among 5 sampling sites was found. For fine particles, the highest $\delta^{15}\text{N}_{\text{THAA}}$ value of fine particles were observed in urban (average= $9.4 \pm 2.5\%$), town (average= $8.4 \pm 1.5\%$), then in the suburban (average= $5.4 \pm 1.1\%$), agricultural area
300 (average= $5.9 \pm 2.8\%$) and forest (average= $5.7 \pm 1.9\%$) sites. For coarse particles, the most positive $\delta^{15}\text{N}_{\text{THAA}}$ value were also occurred in urban (average= $8.6 \pm 0.9\%$), town (average= $7.0 \pm 1.6\%$), then in the suburban (average= $4.3 \pm 3.4\%$), agricultural area (average= $6.0 \pm 3.1\%$) and forest (average= $5.4 \pm 2.6\%$) sites (Fig. 4c). The more positive $\delta^{15}\text{N}_{\text{THAA}}$ values occurred in urban and town compared to other

sampling sites for both fine and coarse particles ($p < 0.05$), indicating that atmospheric AAs for both fine and coarse particles in urban and town were more influenced by biomass burning.

3.4 Different degradation state of AAs between fine and coarse aerosol particles

In this study, a huge difference was observed in the concentrations and mol% compositions of THAAs between fine and coarse particles (Fig. 1 and 3). As we discussed above, the sources of AAs in fine and coarse particles are similar, therefore this larger difference may be attributed to protein matter in fine and coarse undergoing different degrees of oxidation, nitration and oligomerization in the atmosphere (Liu et al., 2017; Wang et al., 2019; Song et al., 2017; Haan et al., 2009). Another possibility is that, biologically relevant degradation of AAs may contribute to this variation observed between fine and coarse particles. To investigate whether AAs in fine and coarse particles may be degraded by bacteria to different degrees, degradation marker (DI) and bacterial heterotrophy indicators ($\delta^{15}\text{N}$ -AA distribution and $\sum V$) were used. Protein as major components in all source organisms are sensitive to all stages of degradation (Cowie and Hedges 1992). Moreover, compared to the alteration of the degradation, the dissimilarity in amino acid composition of protein in the source organisms are minor (Dauwe and Middelburg 1998). Therefore, the degradation index (DI) is developed, which are based on protein amino acid composition and factor coefficients based on the first axis of the PCA analysis (equation 1). Since AAs concentrated in cell walls are preferential accumulated during decomposition, whereas amino acids that are concentrated in cell plasma tend to be depleted during degradation (Dauwe et al., 1999), the compositional changes of amino acids associated with degradation can be traced by the DI value. The higher DI values indicate the protein is relatively “fresh” (Yan et al., 2015) and changes tracked by DI are proposed to be driven in large part by enrichment of AAs concentrated in cell wall (Mccarthy et al., 2007).

For calculation of DI values for fine and coarse particles, the first principal component score from principal component analysis (PCA) was applied to our own data (including Ala, Gly, Val, Leu, Ile, Pro, Ser, Thr, Phe, Asp, Glu, Lys, His and Tyr), following the method described by Dauwe et al. (1999). The first principal component explained 38% of the variability, and the second principal component explained 21% (Table S2). Fig. 5a shows plots of the scores of the first and second principal components of fine and coarse particles in 5 sites. Components of fine and coarse particles could be roughly separated. The plots of the fine particles tended to cluster in the upper middle and right areas (approximately -1.7 to +2.0, and -0.4 to 1.4 at first and second principal component scores, respectively). In contrast, the plots of the coarse particles tended to locate in the lower and left areas (approximately -1.9 to 1.4, and -2.8 to +0.5 at first and second principal component scores, respectively). Fine and coarse particles were clearly distinguished by first principal component scores, suggesting that the first principal component score may also be designed as a degradation index of THAA in aerosols.

This is the first report of the DI values for aerosol particles. We compared DI values obtained by our calculating method with those calculated by using the coefficients given in previous references (Dauwe et al., 1999; Yamashita and Tanoue, 2003). There is no significant difference between the DI values calculated using the first principal component score and the DI values calculated using the coefficients given in the previous reference (Dauwe et al., 1999; Yamashita and Tanoue, 2003) ($p > 0.05$) (Fig. S3), confirming our calculation method is reliable.

A plot of factor coefficients of each individual amino acid in the first and second principal components was examined to clarify the reasons for variation of the scores of fine and coarse particles (Fig. 5b).
345 Based on this cross plot, 14 HAA species were divided into four groups. In Fig. 5b, Group 1 located in the lower right portion of the plot, included Val, Leu, Ile and Ala. Group 2, in the upper right of the plot, included Lys, Glu, Asp, Phe, Thr, Ser and Gly. Group 3, in the middle direction, included Tyr and His. Group 4, in the left of the plot, included Pro. The principal component scores of atmospheric particles were affected by the relative abundance and the factor coefficient of each individual amino acid. The
350 relative high principal component scores of fine particles in PC1 and PC2 were more affected by the high relative abundances of amino acids which has high factor coefficient (Group 1 and Group 2). In contrast, the relative low principal component scores of coarse particles in PC1 and PC2 were more affected by the low relative abundances of amino acids which has low factor coefficient (Group 1 and Group 4).
Furthermore, DI values for fine particles showed positive correlation with percentage of HAA species in
355 Group1 (e.g., Lys, Glu, Asp, Phe, Thr, Ser), but DI values for coarse particles were positively correlated to percentage of HAA species in Group 2 (e.g., Ala, Val, Leu and Ile) (Fig. S4), indicating the difference in composition profiles of HAA between fine and coarse particles may affected by the degradation process. Plots of DI as a function of THAA concentration in both fine and coarse particles showed an exponential relationship ($y=1067.4e^{-1.0x}$; $r=0.6$, $p<0.01$); that was, that at higher values of DI, concentrations of THAA were higher, and vice versa (Fig. S5). The coarse particles had significantly
360 lower THAA concentrations compared to fine particles (Fig. S1). Clearly, both composition profiles of HAA and concentrations of THAAs in aerosols may be related to degradation processes.
DI values from literature data, where possible and DI values for fine and coarse aerosol particles are shown in Fig. 6a and Fig. 7. Fine particles had significantly higher DI values than that of coarse particles
365 ($p<0.05$) (Fig. 6a). The DI values for fine and coarse particles ranged from -0.3 to 1.4 (average= 0.6 ± 0.4) and -1.8 to 1.4 (average= -0.6 ± 1.0), respectively (Fig. 7). The DI values of fine particles were close to those of “fresh” material. For instance, source materials (e.g., plankton, bacteria and sediment trap material). On the contrary, the DI values of coarse particles were comparable to those of surface soil, POM in coastal sediments and DOM in coastal area, which were proved to be more degraded materials
370 (Fig. 7). In marine environment, high DI values (>0.5) indicate the better preservation of more fresh organic matter from marine primary production (Jiang et al., 2014). On the contrary, low DI values (<0.5) indicate the presence of relatively degraded organic matter (Burdige, 2007; Wang et al., 2018). In this study, the lower DI values observed in coarse particles, implying that AAs in coarse particles may undergo more degradation than fine particles. Our result is also comparable to that observed in
375 precipitation at Uljin and Seoul (Yan et al., 2015). The DI values measured in coarse particles are closer to those observed in Seoul, where is believed to have more advanced degradation than Uljin, further supporting the degradation degree of amino acids in coarse particles is higher than that in fine particles. However, the differences in DI values were not significant among 5 sampling sites for both fine and coarse particles ($p>0.05$) (Fig. S6). For fine particles, the average DI values in agricultural area, urban, forest, town and suburban location was 0.6 ± 0.4 , 0.5 ± 0.5 , 0.7 ± 0.3 , 0.6 ± 0.3 and 0.7 ± 0.2 , respectively. For
380 coarse particles, the mean DI values in agricultural area, urban, forest, town and suburban location was -0.5 ± 0.9 , -1.0 ± 1.1 , -0.8 ± 1.1 , -0.3 ± 1.1 and -0.5 ± 1.1 , respectively. As we discussed above, the sources of

atmospheric HAA were different among 5 sampling sites. This result suggested that the degradation process of amino acids in the atmosphere is less affected by their emission sources.

385 **3.5 Bacterial signature in aerosol AAs**

The existence of microorganisms in aerosol particles has been documented. However, whether bacterial degradation processes play a role in atmospheric protein degradation is not well understood. The negative correlation of the DI with the concentration of free γ -aminobutyric acid (GABA) and its mole percentage are depicted in Figure S7. Since bacteria are known to produce free GABA from their protein precursors
390 (Cowie and Hedges 1994; Koolman and Roehme, 2005), the concentrations and mole percentage of free GABA may tend to increase during the biodegradation process. Therefore, negative relationship between the DI values and GABA in aerosol suggested that the degradation of atmospheric protein is probably induced by bacteria. Dauwe et al. (1999) have also reported that the negative correlation of the DI with the mole percentage of the GABA and β -alanine (BALA) in marine particulate matter samples and they
395 attributed the correlation of the DI with the variation of GABA mole percentage to the stimulation of degradation by the activity of microorganism.

Moreover, it is interesting to note that a substantial $\delta^{15}\text{N}$ -AA shifts in trophic AA group was observed between fine and coarse particles among 5 sampling sites. Ala, Leu, Ile and Asp was ^{15}N -enriched in coarse particles compared to fine particles, whereas Pro in coarse particles was ^{15}N -depleted than those
400 in fine particles (Fig. 8). Clearly, there is no uni-directional ^{15}N depletion or enrichment of Trophic-AA was observed between fine and coarse particle samples. The $\delta^{15}\text{N}$ -AA distribution in the Trophic-AA group is more “scattered” in coarse particles than that in fine particles (Fig. 8). However, the difference in $\delta^{15}\text{N}$ values of Source-AA between coarse particles and fine particles was relatively small except for Val. $\delta^{15}\text{N}$ values of Gly, Ser, Phe and Lys measured in coarse particles are close to those measured in fine
405 particles. Recent work on $\delta^{15}\text{N}$ signatures of individual AA has suggested that bacterial heterotrophy often results in strong fractionation in some specific AA, which are tied directly to specific microbial biochemical pathways. Among those specific AA, both Ala and Leu are commonly observed to show strong $\delta^{15}\text{N}$ shifts with the processes of bacterial heterotrophy (McCarthy et al., 2004). Hence, ^{15}N -enriched Ala and Ile founded in coarse particles compared to fine particles suggested more bacterial
410 heterotrophy have taken place in coarse particle.

Heterotrophic reworking of protein encompasses a series of processes including hydrolysis, uptake and de novo synthesis, salvage AA incorporation into new protein. Therefore, new protein reworked by heterotrophically processes represent a mixture of resynthesized AAs and AAs that has never been hydrolyzed (salvaged AAs). McCarthy et al. (2007) hypothesized that the process of incorporating the
415 salvage AAs into new protein should not alter original $\delta^{15}\text{N}$ values of salvage AAs. The substantial $\delta^{15}\text{N}$ -AA shifts in only selected AA indicates the N of an assimilated AA has been replaced through a de novo *heterotrophic* AA resynthesis pathway with N isotope fractionation. Therefore, the substantial $\delta^{15}\text{N}$ -AA shifts in trophic AA group could be observed when bacterial heterotrophy has occurred and those new resynthesized protein has become an important part of protein material measured (Mccarthy et al., 2007).
420 Fogel and Tuross (1999) first observed that $\delta^{15}\text{N}$ -AA patterns of degraded material was highly “scattered” and the N isotope fracination between degraded material and fresh protein were up to 15%. Moreover,

obviously changes for the $\delta^{15}\text{N}$ values of several AA were founded in high molecular weight dissolved organic carbon after bacterial reworking (Calleja et al., 2013). Similarly, the “scattered” characteristic of $\delta^{15}\text{N}$ -AA distribution in Tr-AA group of coarse particles may be due to the nitrogen fractionation occurred in microbial consumers selectively using Trophic-AA.

ΣV is defined as the average deviation in six Trophic-AA and has been proposed to reflect the extent of protein resynthesis during microbial degradation processes (Mccarthy et al., 2007). Fig. 9 shows the ΣV values measured in fine particles, coarse particles, and local natural sources, as well as ΣV values reported in previous references. ΣV values for main natural sources collected around the sampling sites were calculated. ΣV values for local plants (needles of *Pinus massoniana* (Lamb.) and leaves of *Camphora officinarum*) ranged from 1.0‰ to 2.1‰, with a mean of 1.7 ± 0.4 ‰ (Fig. 9). ΣV values in local soil (paddy soil, road soil and forest soil) ranged from 1.4‰ to 2.1‰, with a mean of 1.7 ± 0.3 ‰. Overall, coarse particles had higher ΣV value (average = 3.6 ± 1.5 ‰) than that of fine particles ($p < 0.05$) (Fig. 9). The mean ΣV value of fine particles in 5 sampling sites (average = 2.4 ± 1.1 ‰) was similar to or slightly higher than that of plants and soil collected around sampling sites, phytoplankton (1.0‰) and zooplankton (1.5‰) in marine (Mccarthy et al., 2007), needle (average = 1.5 ± 0.1 ‰), mosses (average = 1.1 ± 0.02 ‰) and soil (average = 1.4 ± 0.1 ‰) measured in balsam fir forest (Philben et al., 2018), and marine POM (average = 2.3 ± 0.7 ‰) (Batista et al., 2014; Mccarthy et al., 2007). In contrast, ΣV values of coarse particles were equal to or even higher than those of more degraded materials, such as marine dissolved organic matter (DOM) reworked by bacterial heterotrophy (average = 3.0 ± 0.5 ‰) (Batista et al., 2014).

ΣV could reflect the increasing trend of “scatting” $\delta^{15}\text{N}$ -Trophic AA pattern related to more intensive bacterial resynthesis (Batista et al., 2014; Calleja et al., 2013; Yamaguchi et al., 2017). In this study, the significant higher values of ΣV were measured in coarse particles than those in fine particles ($p < 0.05$) (Fig. 6). Moreover, the mean ΣV value of fine particles was similar to or slightly higher than that measured in “fresh” materials (Mccarthy et al., 2007; Philben et al., 2018; Batista et al., 2014), while ΣV values of coarse particles were equal to or even higher than those of more degraded materials (Fig. 9). These corroborate that more bacterial heterotrophic resynthesis occurred in coarse particles compared to fine particles.

Despite the uncertainties surrounding oxidation, nitration and oligomerization of AAs in the atmosphere, main observations remain that the difference in $\delta^{15}\text{N}$ values of Source-AA (Gly, Ser, Phe and Lys) and total hydrolysable amino acids ($\delta^{15}\text{N}_{\text{THAA}}$) between coarse particles and fine particles was relatively small (Fig. 3). The average offset of $\delta^{15}\text{N}_{\text{THAA}}$ value between fine and coarse particles was lower than 1.5‰ (Fig. 4a). These results appear to contrast with what one might expect for AAs in either sizes particles undergo particularly more photochemical transformation than the other. Therefore, significantly lower DI values, “scattered” characteristic of $\delta^{15}\text{N}$ distribution in Tr-AA and higher ΣV values observed in coarse particles in this study provide evidence that the difference in the THAA concentration and mol% composition distribution between fine and coarse particles may be related to AAs in coarse particles have stronger bacterial degradation state than those in fine particles.

3.6 Release of coarse “Fresh” bioparticles during the rainfall

A tight relationship between atmospheric bioaerosols and precipitation has been found by previous studies (Huffman et al., 2013; Yue et al., 2016). Since biological sources contain a large abundance of AAs (Ren et al., 2018), HAAs in aerosols can be used as tracer compounds to indicate the release of biological sources during precipitation. However, detailed size-resolved and time-resolved observation
465 for the release of bioparticles initiated by precipitation are sparse and the degradation state of different sizes bioparticles has never been examined.

In this study, precipitation was observed to exert different impacts on the concentrations of the THAA in fine and coarse particles. The average concentration of THAA in fine particles on rainfall days ($1948 \pm 1546 \text{ pmol m}^{-3}$) was significantly lower than that measured on dry days ($3137 \pm 1898 \text{ pmol m}^{-3}$) ($p < 0.05$), whereas the average concentrations of THAA in coarse particles displayed no significant changes
470 during rain events ($p > 0.05$) (Fig. 1 and Fig. S1). For coarse particles, the average concentrations of THAA on rainy and dry days was $660 \pm 947 \text{ pmol m}^{-3}$ and $212 \pm 266 \text{ pmol m}^{-3}$, respectively. It is expected that the concentrations of individual AAs in aerosol were assumed to decrease during rainfall events because of the high scavenging ratio of AAs in aerosol (Gorzelska and Galloway, 1990). In this study,
475 from rain to dry periods, the concentrations of THAA for fine particles decreased ($p < 0.05$) (Fig. S1), but the concentration of THAAs for coarse particles displayed not significant change ($p > 0.05$) (Fig. S1). Similar variation trends of different size particles following the precipitation were also observed by (Huffman et al., 2013). They also found the steep increase of coarse particles while low concentrations of fluorescent bioparticles and total aerosol particles were found in fine particles during the precipitation,
480 suggesting the new released AAs during the precipitation are mainly distributed in coarse particles.

It is worth noting that the influence of precipitation on the mole composition profile of HAA is different for the coarse and fine particles (Fig. 2). For fine particles, only the percentage of Pro significantly increased from $14 \pm 6\%$ on dry days to $20 \pm 9\%$ on rainfall days ($p < 0.05$). There was no apparent trend in the percentage of other individual HAAs for fine particles following the precipitation.

485 For coarse aerosol, the percentage composition of HAA in dry periods is quite different from that in rainy periods for coarse particles (Fig. 2). From dry periods to rainfall periods, the percentage of Pro in coarse particles significantly decreased from $74 \pm 25\%$ to $53 \pm 34\%$ ($p < 0.05$), meanwhile the percentage of Ala, Val, Leu, Ile and Glu in coarse particles significantly increased ($p < 0.05$). These HAA species together accounted for 39% of the total THAA pool during dry periods, while during rainfall events this proportion
490 was only 20%. Besides that, compared to fine particles, the large variation in mole composition of THAA for coarse particles was observed following rain events (Fig. 2). From dry periods to rainfall periods, the percentage changes of Pro for coarse particles (21%) was roughly 4 times greater than that for fine particles (6%). Similarly, from dry periods to rain periods, the increase in the percentage of Ala, Val, Leu, Ile and Glu in coarse particles is significantly greater than that in fine particles. For example, following
495 the precipitation, Val in coarse particles increased by 4%, whereas Val in fine particles only increased by 0.3%. These large variations in the percentage of some HAA species (e.g., Pro, Ala, Val, Leu, Ile and Glu) were observed in coarse particles following the rainfall events, which imply the states of coarse particles measured during rain periods were different from the ones measured during dry periods (Fig. 2).

This conclusion also supported by the variation of DI and $\sum V$ values for coarse particles following rain
500 events. As exhibited in Fig. 6a, DI values of coarse aerosol particles were influenced by precipitation.

For coarse aerosol particles, a significant increase was found from dry (average=-1.0±0.8) to rain periods (average=-0.3±1.1) ($p<0.05$), whereas the DI values of fine particles during dry (average=0.7±0.3) and rain periods (average=0.6±0.4) were not significantly different ($p>0.05$). Fig. 6b shows the $\sum V$ values of fine and coarse particles during dry and rainy days. The $\sum V$ values of coarse aerosol particles were significantly affected by precipitation. From dry to rainy days, $\sum V$ values of coarse aerosol particles decreased from 4.5±1.5‰ to 3.0±1.3‰ ($p<0.05$). In contrast, the average $\sum V$ value of fine particles on dry and rainy days was identical (2.4±1.1‰). From dry to rain periods, DI values in coarse aerosol particles were significant increased ($p<0.05$) but the $\sum V$ value was significantly decreased ($p<0.05$), suggesting more fresh AAs in coarse particles were released during rain events, whereas, on dry days AAs in coarse particles were more degraded.

Furthermore, we observed an obviously temporal variations of the concentration and mol% composition of HAA for coarse particles during the precipitation. The higher concentration of THAAs in coarse particles occurred in April 30, May 5, May 6 and May 13 when daily precipitation amount was higher and duration of rainfall was longer (Fig. 1 and Table S4). Previous studies demonstrated that droplets splashing on porous medium can deliver fresh biological aerosols in porous medium to the aerosol and this mechanism is closely related to the amounts and intensity of the rainfall events (Joung and Buie, 2015; Huffman et al., 2013; Yue et al., 2016). Thus, the temporal variation trend of HAA concentration for coarse particles in this study can attributed to the active release of biological aerosols caused by droplets and it highly depends on the amounts and intensity of the rainfall. Moreover, the mol% composition of HAA in coarse particles measured in the stronger rainfall events were significantly different from that observed in rainfall events with lower precipitation amount amount and shorter rainfall duration (weak rainfall events). Specifically, a steep decrease in the percentage of Pro and increase of other HAAs in coarse particles mainly occurred in the stronger rainfall events, whereas the mol% composition of HAA in the weak rainfall events were similar to that observed on dry days (Fig. 2). As we discussed above, AAs in coarse particles on dry days were more degraded. Therefore, we can conclude that those “fresh” protein matters in coarse particle are prone to release by droplets and amounts and intensity of the rainfall are the key factors controlling this mechanism.

4 Conclusions

This size distribution of AAs can help understand its transformation and fate in the atmosphere. Therefore, verification of the different types, concentrations, origin and atmospheric processes of AAs distribution along the different air particle sizes is important and meaningful.

This study presents the first isotopic evidence that the sources of AAs for fine and coarse aerosol particles may be similar, all of which were influenced by biomass burning, soil, and plant sources. It is therefore that the huge difference in the concentrations and mol% compositions of THAAs between fine and coarse particles observed in this study is closely relevant to the degradation processes of AAs in aerosols.

Although the oxidation, nitrification and oligomerization processes of protein substances in the atmosphere have been widely reported, these abiotic photochemical aging processes that occur between fine particles and coarse particles have not been compared. In this study, the difference in $\delta^{15}\text{N}$ values of

Source-AA (Gly, Ser, Phe and Lys) and total hydrolysable amino acids ($\delta^{15}\text{N}_{\text{THAA}}$) between coarse
540 particles and fine particles was relatively small. The average offset of $\delta^{15}\text{N}_{\text{THAA}}$ value between fine and
coarse particles was lower than 1.5%. These results appear to contrast with what one might expect for
AAs in either sizes particles undergo particularly more photochemical transformation than the other.

On the contrary, the degradation of atmospheric AAs in aerosols is rarely investigated. This is the first
report of using degradation marker (DI) to investigate the degradation state of aerosol particles. Both
545 composition profiles of HAA and concentrations of THAAs in aerosols are showed to be closely related
to DI. And fine particles had significantly higher DI values than that of coarse particles ($p < 0.05$),
suggesting the degradation degree of amino acids in coarse particles is higher than that in fine particles.
Combining new compound-specific nitrogen isotope tool ($\delta^{15}\text{N}$ -HAA) and effective bacterial
heterotrophy indicator (ΣV), “scattered” characteristic of $\delta^{15}\text{N}$ distribution in Tr-AA and higher ΣV
550 values were observed in coarse particles in this study, which firstly provide evidence that the stronger
degradation state the found in coarse particles are coupled with more bacterial heterotrophic resynthesis
occurred in coarse particles.

This study suggests the potentially significant role of bacterial degradation processes in concentration
and composition of protein distribution in size-segregated aerosol particles. Since the degradation state
555 of airborne protein distribution along size-segregated particles is closely linked to its biological
availability, ecological processes and plant nutrition after deposition, further studies of quantitative
assessment of this biological related process in aerosols should be conducted.

Author contributions. Ren-guo, Zhu., Zequn Wen and Yuwen Zhu designed the experiments, performed
560 analyses, and analyzed the data. Hua-Yun Xiao were the principal investigators of the project that
supported this work. All the authors have helped in the discussion of the results and collaborated in
writing this article.

Acknowledgements. This work was supported by the National Natural Science Foundation of China
565 (Grant No.41425014 and 41463007), Key Laboratory Project of Jiangxi Province (20171BCD40010)
and Two 1000 Talents Plan Project of Jiangxi Province (S2018CQKJ0755). We are thankful to Global
Weather and Climate Information Network (<http://www.weatherandclimate.info/>) for providing
meteorological parameters include temperature (T) and relative humidity (RH), during the sampling
period.

570 **References**

- Amato, P., Demeer, F., Melaouhi, A., Fontanella, S., Martin-Biesse, A.-S., Sancelme, M., Laj, P., and
Delort, A.: A fate for organic acids, formaldehyde and methanol in cloud water: their biotransformation
by micro-organisms, *Atmos. Chem. Phys. D.*, 7, 5253-5276, 2007.
- 575 Barbaro, E., Feltracco, M., Cesari, D., Padoan, S., Zangrando, R., Contini, D., Barbante, C., and Gambaro,
A.: Characterization of the water soluble fraction in ultrafine, fine, and coarse atmospheric aerosol, *Sci.
Total Environ.*, 658, 1423-1439, <https://doi.org/10.1016/j.scitotenv.2018.12.298>, 2019.
- Batista, F. C., Ravelo, A. C., Crusius, J., Casso, M. A., and McCarthy, M. D.: Compound specific amino
acid $\delta^{15}\text{N}$ in marine sediments: A new approach for studies of the marine nitrogen cycle, *Geochim.
Cosmochim. Acta*, 142, 553-569, doi:10.1016/j.gca.2014.08.002, 2014.
- 580 Bauer, H., Kasper-Giebl, A., Löflund, M., Giebl, H., Hitzemberger, R., Zibuschka, F., and Puxbaum, H.:
The contribution of bacteria and fungal spores to the organic carbon content of cloud water, precipitation

- and aerosols, *AtmRe*, 64, 109-119, doi:10.1016/S0169-8095(02)00084-4, 2002.
- Bigg, E. K.: Sources, nature and influence on climate of marine airborne particles, *Environ. Chem.*, 4, 155-161, doi:10.1071/EN07001, 2007.
- 585 Bol, R., Ostle, N. J., and Petzke, K. J.: Compound specific plant amino acid $\delta^{15}\text{N}$ values differ with functional plant strategies in temperate grassland, *J. Plant Nutr. Soil Sci.*, 165, 661-667, doi:10.1002/jpln.200290000, 2002.
- Bowers, R. M., Clements, N., Emerson, J. B., Wiedinmyer, C., Hannigan, M. P., and Fierer, N.: Seasonal Variability in Bacterial and Fungal Diversity of the Near-Surface Atmosphere, *Environ. Sci. Technol.*, 47, 12097-12106, doi:10.1021/es402970s, 2013.
- 590 Burdige, D. J.: Preservation of Organic Matter in Marine Sediments: Controls, Mechanisms, and an Imbalance in Sediment Organic Carbon Budgets?, *Chem. Rev.*, 107, 467-485, doi: 10.1021/cr050347q, 2007.
- Calleja, M. L., Batista, F., Peacock, M., Kudela, R., and McCarthy, M. D.: Changes in compound specific $\delta^{15}\text{N}$ amino acid signatures and d / l ratios in marine dissolved organic matter induced by heterotrophic bacterial reworking, *Mar. Chem.*, 149, 32-44, doi:10.1016/j.marchem.2012.12.001, 2013.
- 595 Chikaraishi, Y., Ogawa, N. O., Kashiyama, Y., Takano, Y., Suga, H., Tomitani, A., Miyashita, H., Kitazato, H., and Ohkouchi, N.: Determination of aquatic food-web structure based on compound-specific nitrogen isotopic composition of amino acids, *Limnol. Oceanogr. Methods*, 7, 740-750, doi: 10.4319/lom.2009.7.740, 2009.
- 600 Dauwe, B., and Middelburg, J. J.: Amino Acids and Hexosamines as Indicators of Organic Matter Degradation State in North Sea Sediments, *Limnol. Oceanogr.*, 43, 782-798, doi:10.4319/lo.1998.43.5.0782, 1998.
- Dauwe, B., Middelburg, J. J. L., and Oceanography: Linking Diagenetic Alteration of Amino Acids and Bulk Organic Matter Reactivity, *Limnol. Oceanogr.*, 44, 1809-1814, doi:10.4319/lo.1999.44.7.1809, 1999.
- 605 Després, V., Huffman, J. A., Burrows, S. M., Hoose, C., Safatov, A., Buryak, G., Fröhlich-Nowoisky, J., Elbert, W., Andreae, M., Pöschl, U., and Jaenicke, R.: Primary biological aerosol particles in the atmosphere: a review, *Tellus B Chem Phys Meteorol*, 64, 15598, 10.3402/tellusb.v64i0.15598, 2012.
- 610 Feltracco, M., Barbaro, E., Kirchgeorg, T., Spolaor, A., Turetta, C., Zangrando, R., Barbante, C., and Gambaro, A.: Free and combined L-and D-amino acids in Arctic aerosol, *Chemosphere*, 220, 412-421, doi:10.1016/j.chemosphere.2018.12.147, 2019.
- Filippo, P. D., Pomata, D., Riccardi, C., Buiarelli, F., Gallo, V., and Quaranta, A.: Free and combined amino acids in size-segregated atmospheric aerosol samples, *Atmos. Environ.*, 98, 179-189, doi:10.1016/j.atmosenv.2014.08.069, 2014.
- 615 Gorzelska, K., and Galloway, J. N.: Amine nitrogen in the atmospheric environment over the North Atlantic Ocean, *Global Biogeochem. Cycles*, 4, 309-333, doi:10.1029/GB004i003p00309, 1990.
- Haan, D. O. D., Corrigan, A. L., Smith, K. W., Stroik, D. R., Turley, J. J., Lee, F. E., Tolbert, M. A., Jimenez, J. L., Cordova, K. E., and Ferrell, G. R.: Secondary Organic Aerosol-Forming Reactions of Glyoxal with Amino Acids, *Environ. Sci. Technol.*, 43, 2818-2824, doi:10.1021/es803534f, 2009.
- 620 Huffman, J. A., Prenni, A. J., DeMott, P. J., Pöhlker, C., Mason, R. H., Robinson, N. H., Fröhlich-Nowoisky, J., Tobo, Y., Després, V. R., Garcia, E., Gochis, D. J., Harris, E., Müller-Germann, I., Ruzene, C., Schmer, B., Sinha, B., Day, D. A., Andreae, M. O., Jimenez, J. L., Gallagher, M., Kreidenweis, S. M., Bertram, A. K., and Pöschl, U.: High concentrations of biological aerosol particles and ice nuclei during and after rain, *Atmos. Chem. Phys.*, 13, 6151-6164, doi:10.5194/acp-13-6151-2013, 2013.
- 625 Husárová, S., Vařtilingom, M., Deguillaume, L., Traikia, M., Vinatier, V., Sancelme, M., Amato, P., Matulová, M., and Delort, A.-M.: Biotransformation of methanol and formaldehyde by bacteria isolated from clouds. Comparison with radical chemistry, *Atmos. Environ.*, 45, 6093-6102, doi:10.1016/j.atmosenv.2011.06.035, 2011.
- 630 Jiang, Z., Liu, J., Chen, J., Chen, Q., Yan, X., Xuan, J., and Zeng, J.: Responses of summer phytoplankton community to drastic environmental changes in the Changjiang (Yangtze River) estuary during the past 50 years, *Water Res.*, 54, 1-11, https://doi.org/10.1016/j.watres.2014.01.032, 2014.
- Joung, Y. S., and Buie, C. R.: Aerosol generation by raindrop impact on soil, *Nat. Commun.*, 6, 6083-6083, doi:10.1038/ncomms7083, 2015.
- 635 Kuznetsova, M., Lee, C., and Aller, J.: Characterization of the proteinaceous matter in marine aerosols, *Mar. Chem.*, 96, 359-377, https://doi.org/10.1016/j.marchem.2005.03.007, 2005.
- Leck, C., and Bigg, E. K.: Source and evolution of the marine aerosol—A new perspective, *Geophys. Res. Lett.*, 32, doi: 10.1029/2005gl023651, 2005.
- 640 Leck, C., and Bigg, E. K.: Biogenic particles in the surface microlayer and overlaying atmosphere in the central Arctic Ocean during summer, *Tellus B Chem Phys Meteorol*, 57, 305-316, doi: 10.3402/tellusb.v57i4.16546, 2005.

- Leck, C., and Keith Bigg, E.: Comparison of sources and nature of the tropical aerosol with the summer high Arctic aerosol, *Tellus B Chem Phys Meteorol*, 60, 118-126, doi: 10.1111/j.1600-0889.2007.00315.x, 2008.
- 645 Liu, F., Lai, S., Tong, H., Lakey, P. S. J., Shiraiwa, M., Weller, M. G., Pöschl, U., and Kampf, C. J.: Release of free amino acids upon oxidation of peptides and proteins by hydroxyl radicals, *Anal. Bioanal. Chem.*, 409, 2411-2420, doi:10.1007/s00216-017-0188-y, 2017.
- Mace, K. A., Artaxo, P., and Duce, R. A.: Water-soluble organic nitrogen in Amazon Basin aerosols during the dry (biomass burning) and wet seasons, *J. Geophys. Res.-Atmos*, 108, doi:10.1029/2003JD003557, 2003.
- 650 Matos, J. T. V., Duarte, R. M. B. O., and Duarte, A. C.: Challenges in the identification and characterization of free amino acids and proteinaceous compounds in atmospheric aerosols: A critical review, *Trends Analyt Chem*, 75, 97-107, doi:10.1016/j.trac.2015.08.004, 2016.
- McClelland, J. W., and Montoya, J. P.: Trophic relationships and the nitrogen isotopic composition of amino acids in plankton, *Ecol.*, 83, 2173-2180, doi: 10.2307/3072049, 2002.
- 655 McCarthy, M. D., Benner, R., Lee, C., Hedges, J. I., and Fogel, M. L.: Amino acid carbon isotopic fractionation patterns in oceanic dissolved organic matter: an unaltered photoautotrophic source for dissolved organic nitrogen in the ocean?, *Mar. Chem.*, 92, 123-134, doi:10.1016/j.marchem.2004.06.021, 2004.
- 660 McCarthy, M. D., Benner, R., Lee, C., and Fogel, M. L.: Amino acid nitrogen isotopic fractionation patterns as indicators of heterotrophy in plankton, particulate, and dissolved organic matter, *Geochim. Cosmochim. Acta*, 71, 4727-4744, doi:10.1016/j.gca.2007.06.061, 2007.
- McCarthy, M. D., Lehman, J., and Kudela, R.: Compound-specific amino acid $\delta^{15}\text{N}$ patterns in marine algae: Tracer potential for cyanobacterial vs. eukaryotic organic nitrogen sources in the ocean, *Geochim. Cosmochim. Acta*, 103, 104-120, doi:10.1016/j.gca.2012.10.037, 2013.
- 665 Papastefanou, C.: Residence time of tropospheric aerosols in association with radioactive nuclides, *Appl. Radiat. Isot.*, 64, 93-100, doi:10.1016/j.apradiso.2005.07.006, 2006.
- Philben, M., Billings, S. A., Edwards, K. A., Podrebarac, F. A., van Biesen, G., and Ziegler, S. E.: Amino acid $\delta^{15}\text{N}$ indicates lack of N isotope fractionation during soil organic nitrogen decomposition, *Biogeochemistry*, 138, 69-83, doi:10.1007/s10533-018-0429-y, 2018.
- 670 Ren, L., Bai, H., Yu, X., Wu, F., Yue, S., Ren, H., Li, L., Lai, S., Sun, Y., and Wang, Z.: Molecular composition and seasonal variation of amino acids in urban aerosols from Beijing, China, *AtmRe*, 203, 28-35, doi:10.1016/j.atmosres.2017.11.032, 2018.
- Samy, S., Robinson, J., Rumsey, I. C., Walker, J. T., Hays, M. D., Robinson, J., Rumsey, I. C., and Hays, M. D.: Speciation and trends of organic nitrogen in southeastern U.S. fine particulate matter (PM_{2.5}), *J. Geophys. Res.-Atmos*, 118, 1996-2006, doi:10.1029/2012JD017868, 2013.
- 675 Song, T., Wang, S., Zhang, Y., Song, J., Liu, F., Fu, P., Shiraiwa, M., Xie, Z., Yue, D., Zhong, L., Zheng, J., and Lai, S.: Proteins and Amino Acids in Fine Particulate Matter in Rural Guangzhou, Southern China: Seasonal Cycles, Sources, and Atmospheric Processes, *Environ. Sci. Technol.*, 51, 6773-6781, doi:10.1021/acs.est.7b00987, 2017.
- 680 Wang, K., Chen, J. F., Jin, H. Y., Li, H. L., and Zhang, W. Y.: Organic matter degradation in surface sediments of the Changjiang estuary: Evidence from amino acids, *Sci. Total Environ.*, 637, 1004-1013, doi:10.1016/j.scitotenv.2018.04.242, 2018.
- Wang, S., Song, T., Shiraiwa, M., Song, J., Ren, H., Ren, L., Wei, L., Sun, Y., Zhang, Y., Fu, P., and Lai, S.: Occurrence of Aerosol Proteinaceous Matter in Urban Beijing: An Investigation on Composition, Sources, and Atmospheric Processes During the "APEC Blue" Period, *Environ. Sci. Technol.*, 53, 7380-7390, doi:10.1021/acs.est.9b00726, 2019.
- 685 Wedyan, M. A., and Preston, M. R.: The coupling of surface seawater organic nitrogen and the marine aerosol as inferred from enantiomer-specific amino acid analysis, *Atmos. Environ.*, 42, 8698-8705, doi:10.1016/j.atmosenv.2008.04.038, 2008.
- 690 Wei, K., Zou, Z., Zheng, Y., Li, J., Shen, F., Wu, C.-y., Wu, Y., Hu, M., and Yao, M.: Ambient bioaerosol particle dynamics observed during haze and sunny days in Beijing, *Sci. Total Environ.*, 550, 751-759, doi:10.1016/j.scitotenv.2016.01.137, 2016.
- Wei, M., Xu, C., Xu, X., Zhu, C., Li, J., and Lv, G.: Characteristics of atmospheric bacterial and fungal communities in PM_{2.5} following biomass burning disturbance in a rural area of North China Plain, *Sci. Total Environ.*, 651, 2727-2739, doi:10.1016/j.scitotenv.2018.09.399, 2019.
- 695 Xu, Y., Wu, D., Xiao, H., and Zhou, J.: Dissolved hydrolyzed amino acids in precipitation in suburban Guiyang, southwestern China: Seasonal variations and potential atmospheric processes, *Atmos. Environ.*, 2019.
- 700 Yamaguchi, Y. T., Chikaraishi, Y., Takano, Y., Ogawa, N. O., Imachi, H., Yokoyama, Y., and Ohkouchi, N.: Fractionation of nitrogen isotopes during amino acid metabolism in heterotrophic and

- chemolithoautotrophic microbes across Eukarya, Bacteria, and Archaea: Effects of nitrogen sources and metabolic pathways, *Org. Geochem.*, 111, 101-112, doi:10.1016/j.orggeochem.2017.04.004, 2017.
- 705 Yamashita, Y., and Tanoue, E.: Distribution and alteration of amino acids in bulk DOM along a transect from bay to oceanic waters, *Mar. Chem.*, 82, 145-160, doi:10.1016/S0304-4203(03)00049-5, 2003.
- Yan, G., Kim, G., Kim, J., Jeong, Y.-S., and Kim, Y. I.: Dissolved total hydrolyzable enantiomeric amino acids in precipitation: Implications on bacterial contributions to atmospheric organic matter, *Geochim. Cosmochim. Acta*, 153, 1-14, doi:10.1016/j.gca.2015.01.005, 2015.
- 710 Yue, S., Ren, H., Fan, S., Sun, Y., Wang, Z., and Fu, P.: Springtime precipitation effects on the abundance of fluorescent biological aerosol particles and HULIS in Beijing, *J. Sci. Res.*, 6, 29618, doi:10.1038/srep29618, 2016.
- Zhang, Q., Anastasio, C., and Jimenez-Cruz, M.: Water-soluble organic nitrogen in atmospheric fine particles (PM_{2.5}) from northern California, *J. Geophys. Res.-Atmos*, 107, AAC 3-1-AAC 3-9, doi:10.1029/2001JD000870, 2002.
- 715 Zhang, Q., Anastasio, C., Free and combined amino compounds in atmospheric fine particles (PM_{2.5}) and fog waters from Northern California, *Atmos. Environ.*, 37, 2247-2258, doi: 10.1016/S1352-2310(03)00127-4, 2003.
- Zhu, R.-g., Xiao, H.-Y., Zhang, Z., and Lai, Y.: Compound-specific $\delta^{15}\text{N}$ composition of free amino acids in moss as indicators of atmospheric nitrogen sources, *J. Sci. Res.*, 8, 14347, doi:10.1038/s41598-018-32531-x, 2018.
- 720 Zhu, R.-g., Xiao, H.-Y., Zhu, Y., Wen, Z., Fang, X., and Pan, Y.: Sources and Transformation Processes of Proteinaceous Matter and Free Amino Acids in PM_{2.5}, *J. Geophys. Res.-Atmos*, 125, e2020JD032375, doi:10.1029/2020jd032375, 2020.

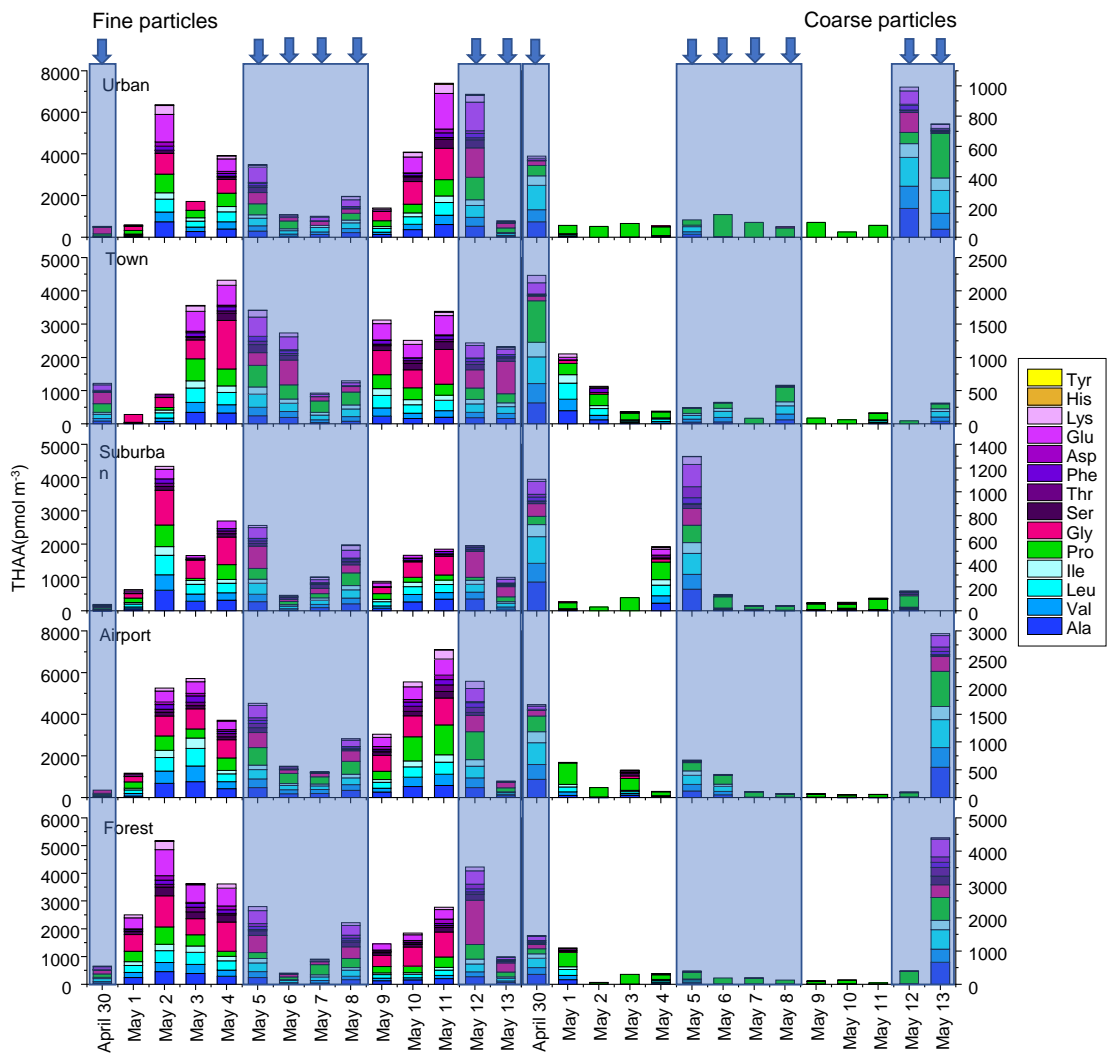


Figure 1. Concentrations of hydrolyzed amino acids for fine and coarse particles in urban, town, suburban, airport and forest sites during 14 consecutive sampling days. The concentrations of HAAs for each sample were normalized for the total volume of air sampled. The blue arrow and shallow represent precipitation.

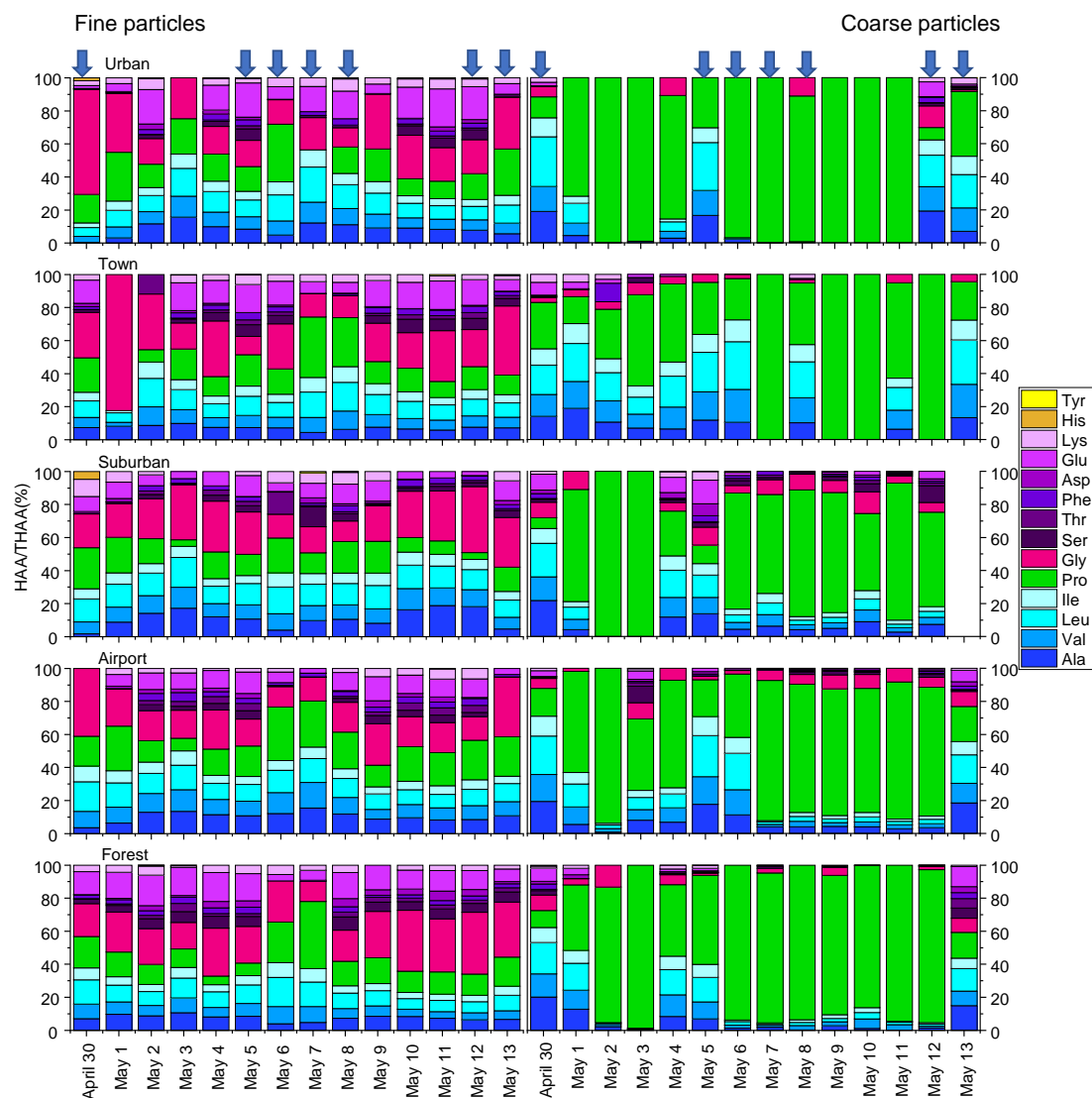


Figure 2. Percentage composition of each hydrolyzed amino acids (% of THAA) for fine and coarse aerosol particles in urban, town, suburban, airport and forest sites during 14 consecutive sampling days. The blue arrow represent precipitation.

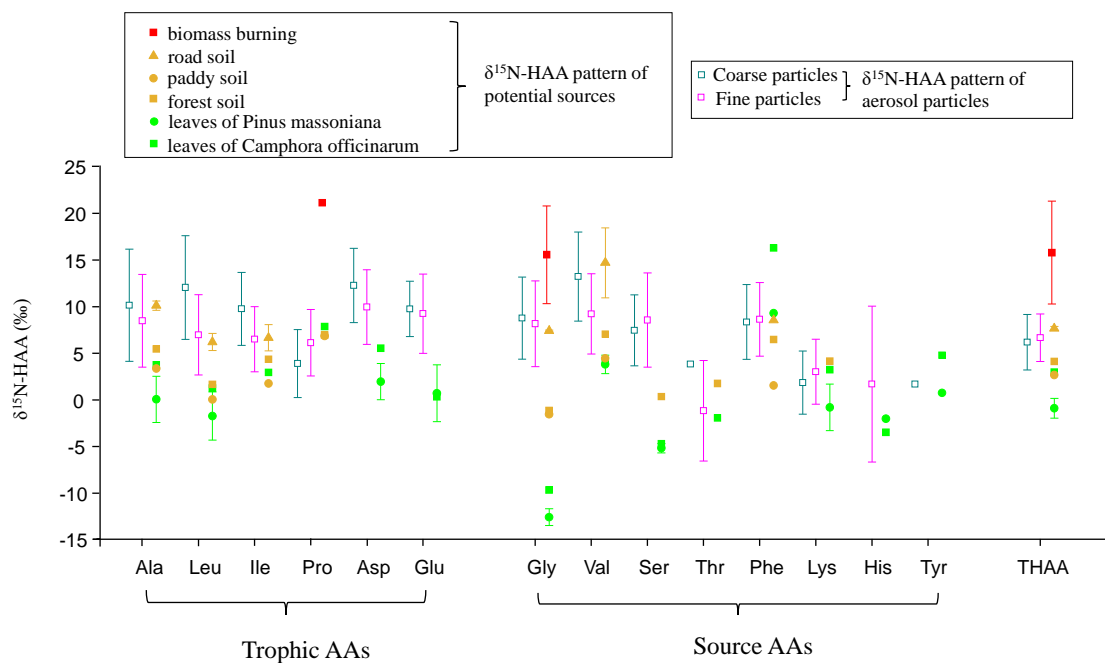


Figure 3. Comparison of $\delta^{15}\text{N-HAA}$ patterns of fine and coarse aerosol particles with that of potential local sources.

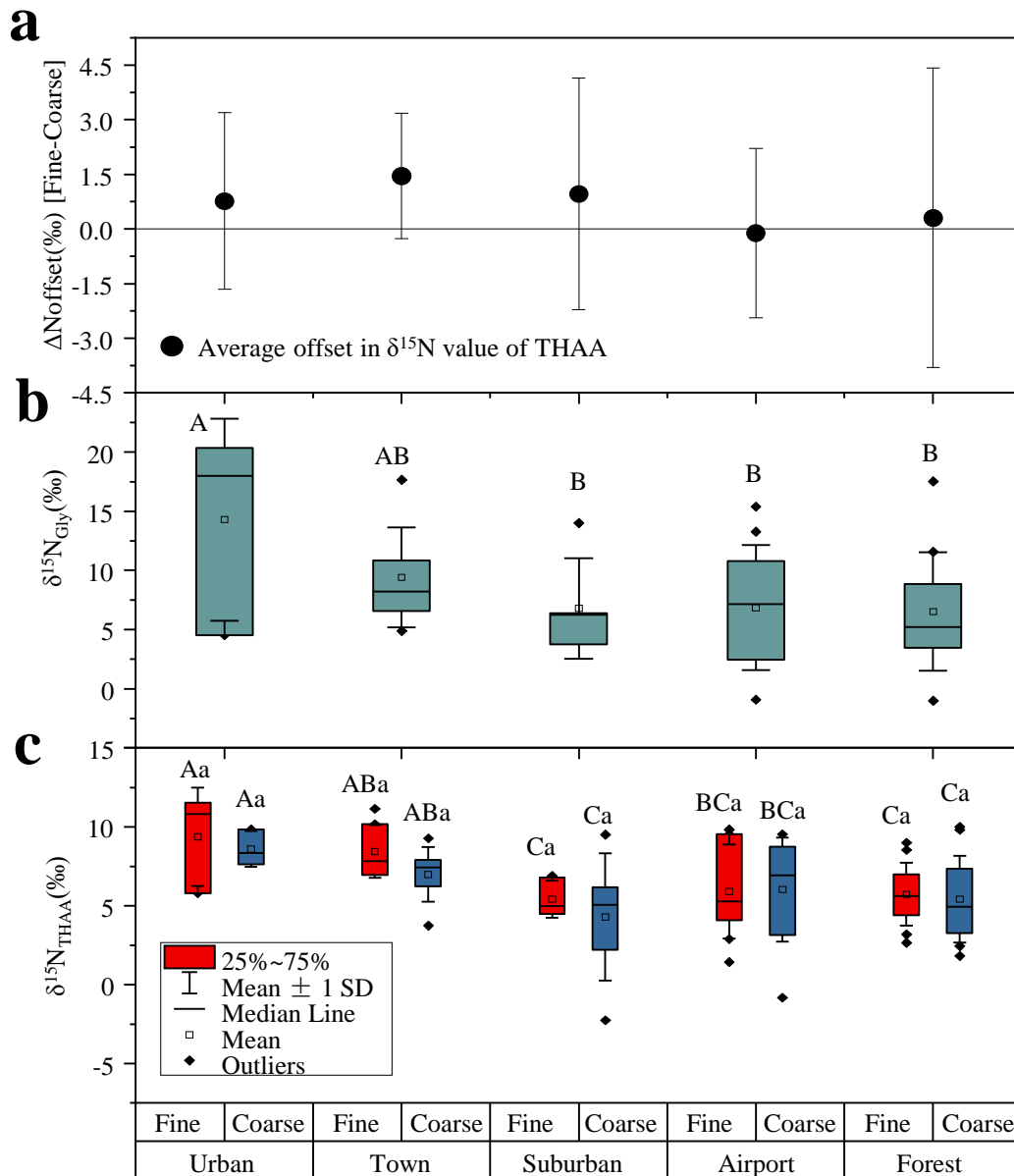


Figure 4. (a) The Offset of $\delta^{15}\text{N}_{\text{THAA}}$ values between fine and coarse particles; (b) The $\delta^{15}\text{N}_{\text{Gly}}$ values of fine particles; (c) The $\delta^{15}\text{N}_{\text{THAA}}$ values of fine and coarse particles in urban, town, suburban, airport and forest sites. Different uppercase letters denote means found to be statistically different (Tukey-HSD test) between sites. Different lower case letters denote a significant difference between fine and coarse particles. The error bars in (a) indicate the standard deviation.

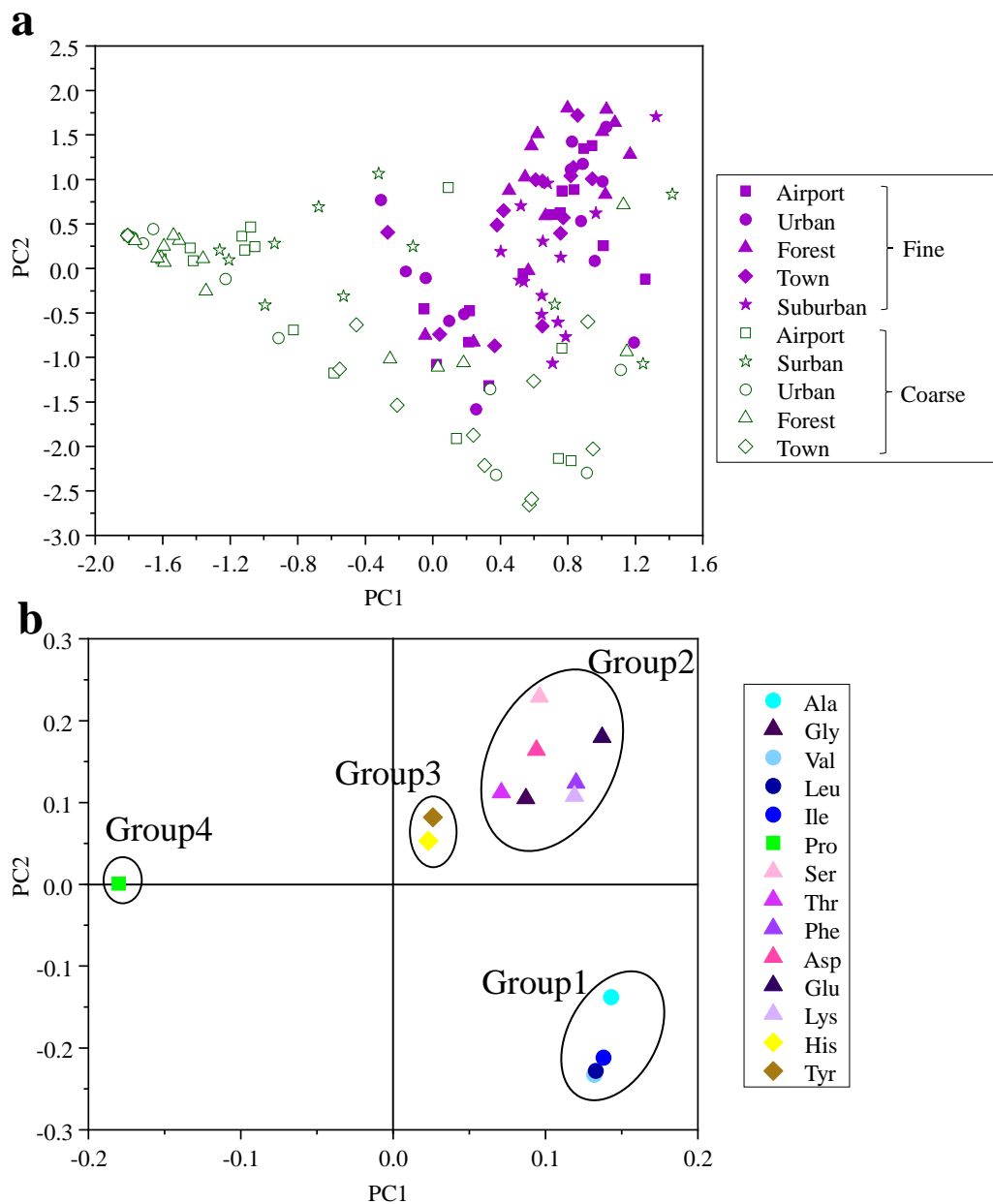


Figure 5. (a) Cross plot of the first and second component scores of PCA based on percentage composition (mol%) of hydrolyzed amino acid for fine and coarse particles. (b) Cross plot of factor coefficients of the first and second principal components of PCA. The lines enclosing each group of amino acid are arbitrarily drawn.

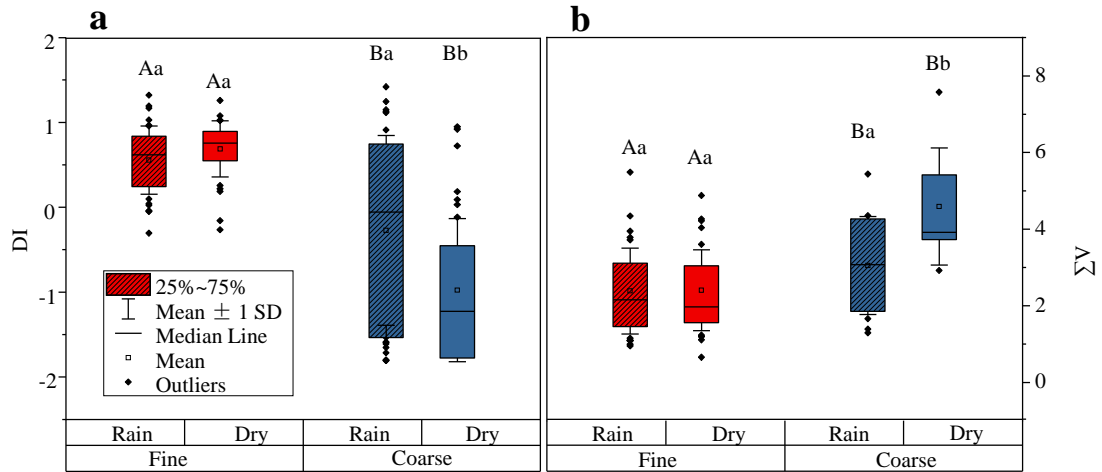


Figure 6. DI values (a) and (b) ΣV for fine (red box) and coarse (blue box) particles. The box encloses 50% of the data, the whisker is standard deviation of the data, the horizontal bar is the median, solid circles are outliers. The differences in means were statistically significant (two-way ANOVA, $p < 0.05$). Different uppercase letters denote means found to be statistically different (Tukey-HSD test) between fine and coarse particles. Different lower case letters denote means found to be statistically different (Tukey-HSD test) between rainy and dry days.

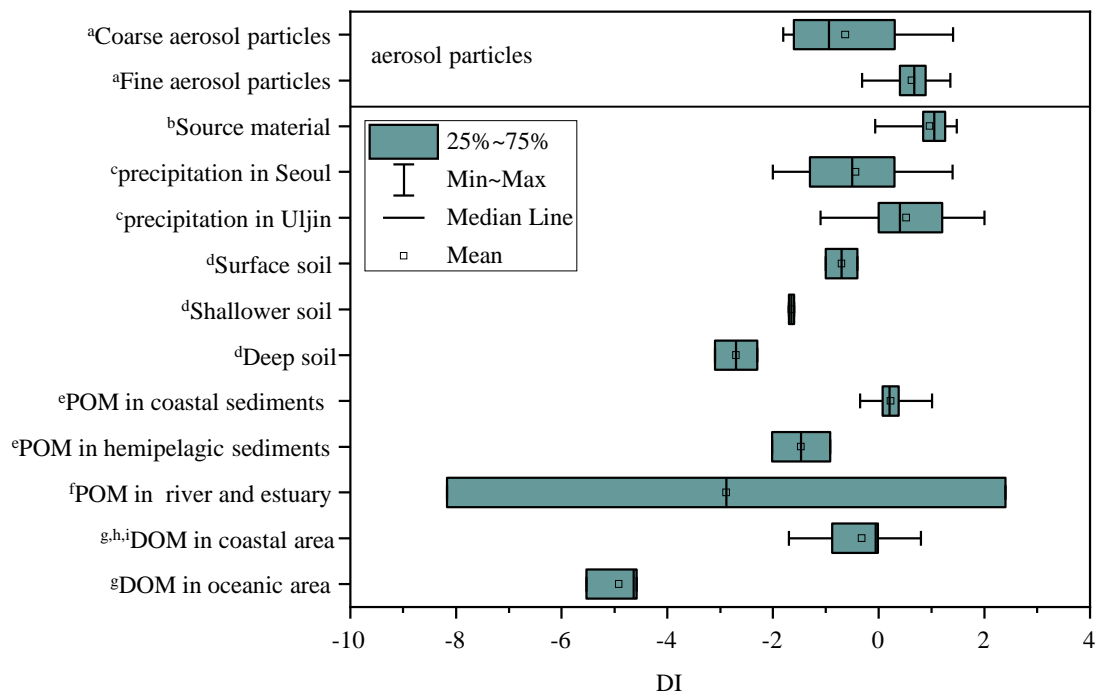


Figure 7. DI values of fine and coarse particles in comparison to other studies. a: this study. b: source materials including phytoplankton, bacteria, zooplankton and sediment trap material from Dauwe et al., 1999. c: Yan et al., 2015. d: Philben et al., 2015. e: particle organic matter from Mccarthy et al., 2007. f: Wang et al., 2018. g: Yamashita and Tanoue, 2003. h: Chen et al., 2016. i: Ji et al., 2019.

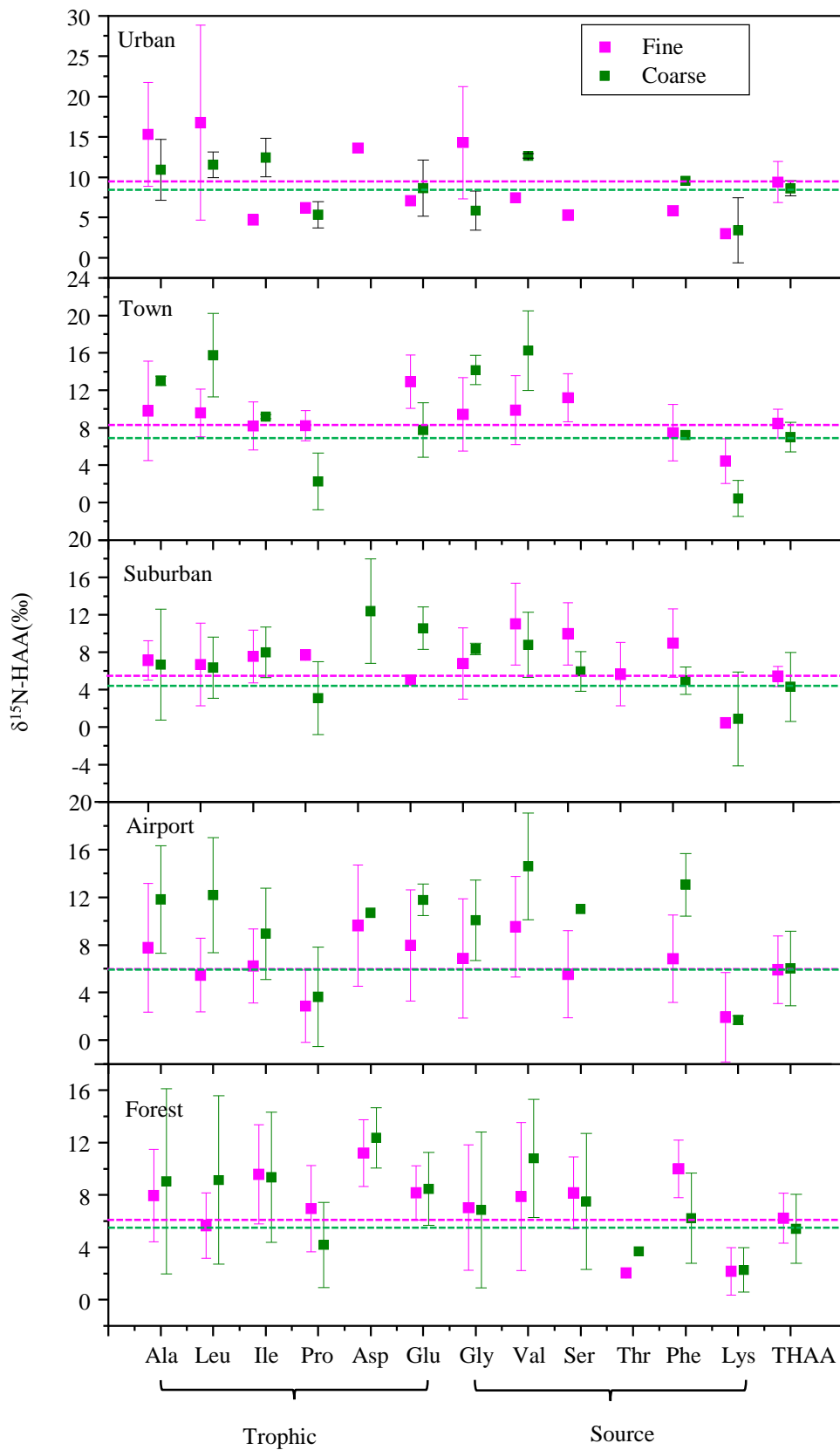


Figure 8. $\delta^{15}\text{N-HAA}$ patterns of fine and coarse aerosol particles in urban, town, suburban, airport and forest sites.

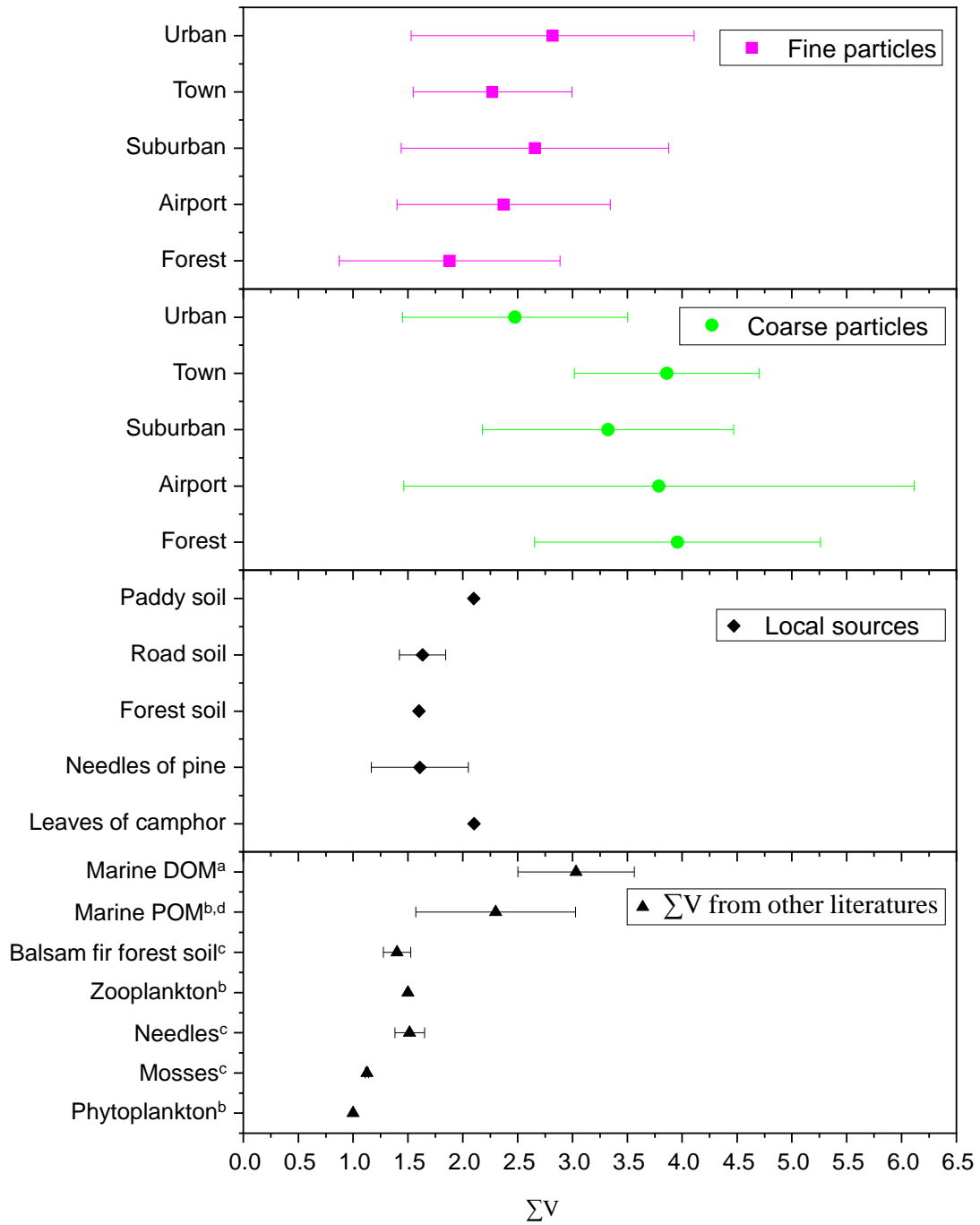


Figure 9. ΣV values for fine and coarse particles in comparison to local natural sources and other studies. a: Calleja et al., 2013. b: Mccarthy et al., 2007. c: Philben et al., 2018. d: Batista et al., 2014.